Structure of GTP-specific succinyl-CoA synthetase in complex with CoA

Ji Huang, Manpreet Malhi,‡ Jan Deneke§ and Marie Elizabeth Fraser*

Department of Biological Sciences, University of Calgary, 2500 University Drive NW, Calgary, AB T2N 1N4, Canada. *Correspondence e-mail: frasm@ucalgary.ca

Edited by B. Hazes, University of Alberta, Canada

‡ Current address: Research Institute, Hospital for Sick Children, Toronto, ON M5G 1X8, Canada.
§ Current address: ProZyme Inc., 3832 Bay Centre Place, Hayward, CA 94545, USA.

Pig GTP-specific succinyl-CoA synthetase is an $\alpha\beta$-heterodimer. The crystal structure of the complex with the substrate CoA was determined at 2.1 Å resolution. The structure shows CoA bound to the amino-terminal domain of the α-subunit, with the free thiol extending from the adenine portion into the site where the catalytic histidine residue resides.

1. Introduction

Succinyl-CoA synthetase (SCS; also known as succinate-CoA ligase) is responsible for breaking down succinyl-CoA to succinate and CoA, accompanied by the phosphorylation of NDP (ADP or GDP) to NTP (ATP or GTP) in the citric acid cycle (Sanadi *et al.*, 1956): succinyl-CoA + NDP + P_i $\rightleftharpoons$ succinate + CoA + NTP. The reaction catalyzed by SCS is reversible and its direction depends on the relative concentrations of the substrates and products. The reverse direction to that occurring in the citric acid cycle produces succinyl-CoA, which may be used for activating ketone bodies (Ottaway *et al.*, 1981) and haem synthesis (Bishop *et al.*, 2012).

In mammals, SCS is a heterodimer and is located within the mitochondria. Two different isoforms exist: one is ATP-specific (ATPSCS; EC 6.2.1.5) and the other is GTP-specific (GTPSCS; EC 6.2.1.4). It was proposed that the different isoforms would be functional in different metabolic pathways (Hamilton & Ottaway, 1981). The two isoforms have the same α-subunit but different β-subunits, and the β-subunit determines the nucleotide specificity (Johnson *et al.*, 1998). In humans, the amount of ATP-specific and GTP-specific SCS varies in different tissues: ATPSCS is more highly expressed in heart, brain and skeletal muscle tissues, while GTPSCS predominates in kidney and liver (Lambeth *et al.*, 2004). SCS deficiency can be caused by mutations of the genes coding for SCS. The three genes are *SUCLG1*, which codes for the α-subunit, *SUCLG2*, which codes for the β-subunit of GTPSCS, and *SUCLA2*, which codes for the β-subunit of ATPSCS. A mutation in *SUCLA2* leading to encephalomyopathy and mitochondrial DNA depletion was first identified in 2005 (Elpeleg *et al.*, 2005).

The interactions between GTP or GDP and the nucleotide-binding site of GTPSCS were revealed using crystals of the nucleotides complexed with pig GTPSCS (Fraser *et al.*, 2006). The nucleotide binds in the ATP-grasp fold (Murzin, 1996) in the amino-terminal domain of the β-subunit, ~30 Å from the histidine residue (His259α) that is phosphorylated transiently in the catalytic reaction. The phosphohistidine loop has been postulated to flip between the nucleotide-binding site and the site where CoA and succinate are proposed to bind, trans-
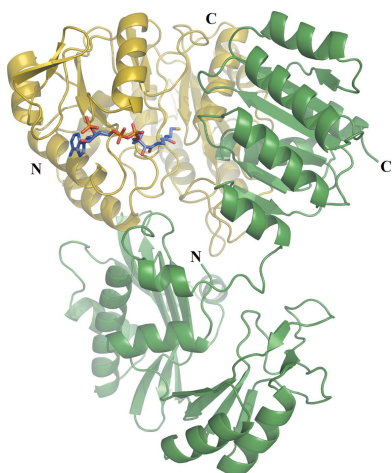
Table 1
Macromolecule-production information.

Source organism	*Sus scrofa*
Oligonucleotide JD1.1 (SpeI site underlined)	GAAAAGAGGAAGATGCTACTAGTGCAAAACGAAT-GAG
Oligonucleotide JD1.2 (SpeI site underlined)	CTCATTCGTTTTGCACTAGTAGCATCTTCCTCTT-TTC
Oligonucleotide JD1.3 (His6 tag underlined)	GATCCCGCCGGTCGCTTAAGTTTATTTATTTAAT-GGTGGTGATGGTGATGCA
Oligonucleotide JD1.4 (His6 tag underlined)	CTAGTGCATCACCATCACCACCATTAAATAAATA-AACTTAAGCGACCGGCGG
Expression vector	pT7-7
Expression host	*E. coli* BL21(DE3)
Complete amino-acid sequence of the construct produced	
Succinyl-CoA ligase (ADP/GDP-forming) subunit α, mitochondrial	SYTASRKHLYVDKNTKVICQGFTGKQGTFHSQQA-LEYGTNLVGGTTPGKGGKTHLGLPVFNTVKEA-KEQTGATASVIYVPPPFAAAAINEAIDAEVPL-VVCITEGIPQQDMVRVKHRLLRQGKTRLIGPN-CPGVINPGECKIGIMPGHIHKKGRIGIVSRSG-TLTYEAVHQTTQVGLGQSLCVGIGGDPFNGTD-FTDCLEIFLNDPATEGIILIGEIGGNAEENAA-EFLKQHNSGPKSKPVVSFIAGLTAPPGRRMGH-AGAIIAGGKGGAKEKITALQSAGVVVSMSPAQ-LGTTIYKEFEKRKMLLVHHHHHH
Succinyl-CoA ligase (ADP/GDP-forming) subunit β, mitochondrial	MNLQEYQSKKLMSDNGVKVQRFFVADTANEALEA-AKRLNAKEIVLKAQILAGGRGKGVFSSGLKGG-VHLTKDPEVVGQLAKQMIGYNLATKQTPKEGV-KVNKVMVAEALDISRETYLAILMDRSCNGPVL-VGSPQGGVDIEEVAASNPELIFKEQIDIIGIK-DSQAQRMAENLGFLGPLQNQAADQIKKLYNLF-LKIDATQVEVNPFGETPEGQVVCFDAKINFDD-NAEFRQKDIFAMDDKSENEPIENEAAKYDLKY-IGLDGNIACFVNGAGLAMATCDIIFLNGGKPA-NFLDLGGGVKESQVYQAFKLLTADPKVEAILV-NIFGGIVNCAIIANGITKACRELELKVPLVVR-LEGTNVHEAQNILTNSGLPITSAVDLEDAAKK-AVASVTKK

Table 2
Crystallization.

Method	Hanging-drop vapour diffusion
Plate type	VDX
Temperature (K)	294
Protein concentration (mg ml^{-1})	7
Buffer composition of protein solution	0.6 mM CoA, 10 mM Tris–HCl, 5 mM β-ME pH 8.0
Composition of reservoir solution for initial microcrystals	1.8 M ammonium sulfate, 1 mM β-ME, 50 mM sodium/potassium phosphate pH 7.0
Composition of reservoir solution for seeding	1.6 M ammonium sulfate, 1 mM β-ME, 50 mM sodium/potassium phosphate pH 7.0
Volume and ratio of drop	1 µl, 1:1
Volume of reservoir (ml)	1

Table 3
Data collection and processing.

Values in parentheses are for the outer shell.

Diffraction source	20 mm asymmetric hybrid small-gap in-vacuum undulator, CLS beamline 08ID-1
Wavelength (Å)	0.97795
Temperature (K)	100
Detector	Rayonix MX-300 CCD
Crystal-to-detector distance (mm)	250
Rotation range per image (°)	0.5
Total rotation range (°)	150
Exposure time per image (s)	1
Space group	$P2_1$
a, b, c (Å)	86.34, 82.50, 49.38
α, β, γ (°)	90, 104.25, 90
Mosaicity (°)	1.2
Resolution range (Å)	41.40–2.10 (2.21–2.10)
Total No. of reflections	114697 (15619)
No. of unique reflections	36903 (5192)
Completeness (%)	94.6 (91.6)
Multiplicity	3.1 (3.0)
$\langle I/\sigma(I)\rangle$	5.9 (2.6)
$R_{\mathrm{r.i.m.}}$†	0.140 (0.556)
Overall B factor from Wilson plot (Å^2)	25.37‡

† Estimated $R_{\mathrm{r.i.m.}} = R_{\mathrm{merge}}[N/(N-1)]^{1/2}$, where N is the data multiplicity. ‡ There are two spikes at 2.25 and 2.17 Å. The fit of the curve used to estimate the B factor is better at lower resolution, >2.8 Å, than at high resolution.

porting the phosphoryl group between the two sites (Fraser *et al.*, 1999). Although the CoA-binding site for GTPSCS has never been analyzed, it is predicted to lie in the amino-terminal domain of the α-subunit based on the structure of the complex of CoA with *E. coli* SCS (Wolodko *et al.*, 1994). In this work, the crystal structure of the complex of CoA with pig GTPSCS, determined at 2.1 Å resolution, is described.

2. Materials and methods

2.1. Macromolecule production

The pT7-7 expression plasmid for GTPSCS has been described previously (Fraser *et al.*, 2006). For ease of purification, a His$_6$ tag was added to the carboxy-terminus of the α-subunit. In conjunction with this addition, a long untranslated region left from the cDNA cloning was removed from the plasmid. To do this, the plasmid was first modified to include an SpeI site (oligonucleotides JD1.1 and JD1.2; Table 1), and this site and an existing BamHI site were used for cleavage. The resulting fragments were separated on an agarose gel and the fragment that included the genes for GTPSCS was extracted from the gel. Pre-annealed oligonucleotides (JD1.3 and JD1.4; Table 1) containing the codons for six histidine residues and the stop codon TAA were ligated to the purified fragment. The sequence was confirmed and this modified expression plasmid was transformed into *Escherichia*

coli BL21(DE3) cells. 100 ml Luria–Bertani broth (2.5 g mix from Life Technologies) containing 100 µg ml^{-1} ampicillin was inoculated with a single colony and the culture was grown overnight with shaking at 225 rev min^{-1} and 37°C. 1 l Terrific Broth (12 g tryptone, 24 g yeast extract, 4 ml glycerol, 2.31 g KH$_2$PO$_4$, 12.54 g K$_2$HPO$_4$ per litre) was inoculated with 50 ml overnight culture and the culture was grown at 37°C and 225 rev min^{-1} to an optical density OD$_{600\,\mathrm{nm}}$ of 1.6–2.0. Protein overproduction was induced with 1.0 mM isopropyl β-D-1-thiogalactopyranoside and the temperature was lowered to 25°C. After 16 h, the cells were harvested by centrifugation for 30 min at 2663g and 4°C. The cells were stored at −80°C in lysis buffer consisting of 20 mM imidazole, 300 mM NaCl, 50 mM NaH$_2$PO$_4$, 5 mM β-mercaptoethanol (β-ME) pH 8.0.

GTPSCS was purified using affinity and gel-filtration chromatography. With the exception of the gel-filtration step, the sample was maintained at 4°C during purification. Frozen cells were thawed on ice and lysed by sonication. Cell debris was

separated by centrifugation at 11 235g for 30 min. The soluble fraction was loaded onto a column containing 10 ml nickel–nitrilotriacetic acid agarose (Qiagen) and washed with 20 mM imidazole, 300 mM NaCl, 50 mM NaH$_2$PO$_4$, 5 mM β-ME pH 8.0. The bound protein was eluted with 100 mM imidazole, 300 mM NaCl, 50 mM NaH$_2$PO$_4$, 5 mM β-ME pH 8.0 and precipitated with 0.5 g ammonium sulfate per millilitre of sample. The precipitate was collected by centrifugation at 7802g for 30 min, redissolved in a minimal volume of buffer and then injected onto a Superdex 200 prep-grade column (GE Healthcare; 1.6 × 62 cm) pre-equilibrated with the same buffer: 50 mM NaH$_2$PO$_4$, 150 mM NaCl, 5 mM β-ME pH 8.0. Pooled fractions were concentrated and exchanged into buffer consisting of 10 mM Tris–HCl, 5 mM β-ME pH 8.0. Previous work showed that the starting methionine is cleaved from the α-subunit (Table 1; Fraser *et al.*, 2006). The concentration of purified GTPSCS was determined using an $A_{280\,nm}(0.1\%)$ value of 0.35 A mg^{-1} cm^{-1} (Murakami & Nishimura, 1974). 20 µl aliquots were flash-frozen in thin-walled PCR tubes in liquid nitrogen and stored at −80°C (Deng *et al.*, 2004). The final yield was ∼2 mg purified GTPSCS per litre of culture.

2.2. Crystallization

The hanging-drop vapour-diffusion technique was used for co-crystallization of the complex of GTPSCS and CoA. Crystallization conditions were based on those used to crystallize GTPSCS in the absence of CoA (Fraser *et al.*, 2000). A
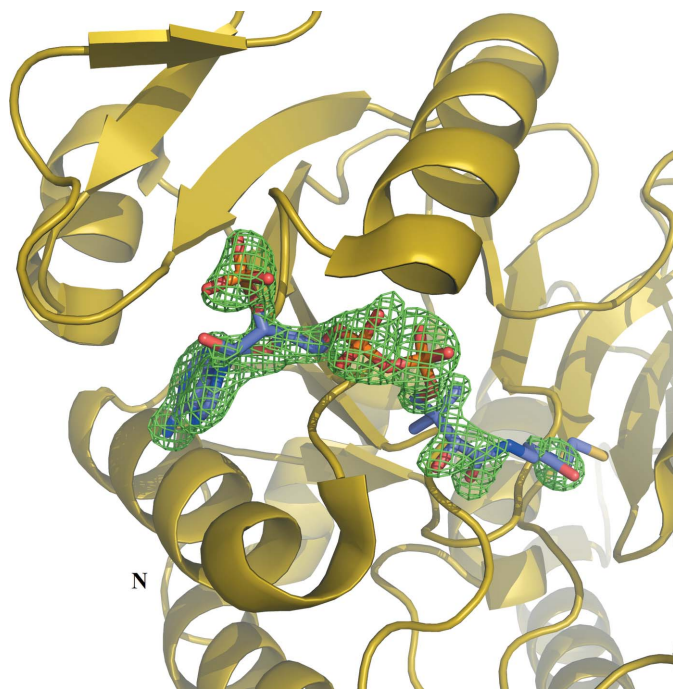
Table 4
Structure refinement.

Values in parentheses are for the outer shell.

Resolution range (Å)	41.40–2.10 (2.175–2.100)
Completeness (%)	93.92 (90.68)
σ Cutoff	None
No. of reflections, working set	33256
No. of reflections, test set	3584
Final R_{cryst}	0.185 (0.274)
Final R_{free}	0.230 (0.344)
No. of non-H atoms	
Protein	5211
CoA	48
Other ligands (phosphate, sulfate, glycerol)	53
Solvent	193
Total	5505
R.m.s. deviations	
Bonds (Å)	0.002
Angles (°)	0.611
Average B factors (Å^2)	
Protein	31.8
CoA	26.4
Other ligands (phosphate, sulfate, glycerol)	42.4
Solvent	31.3
Ramachandran plot	
Favoured regions (%)	98
Outliers (%)	0.14

bundle of crystals was visible within days under the conditions described in Table 2. Crystals from the bundle were crushed to form a seed stock. A single crystal was grown by microseeding after a 10^3-fold dilution of the stock.

2.3. Data collection and processing

Diffraction data were collected on beamline 08ID-1 (CMCF-ID) at the Canadian Light Source (CLS), Saskatoon, Saskatchewan, Canada. Crystals were cryoprotected in solution consisting of 30%(v/v) glycerol, 1.6 M ammonium sulfate, 80 mM sodium/potassium phosphate pH 7.0 and mounted in loops before flash-cooling in nitrogen gas at 100 K and storage in liquid nitrogen for shipment to the synchrotron. Diffraction data were processed using *iMosflm* (Battye *et al.*, 2011) and other programs from the *CCP*4 package (Winn *et al.*, 2011; Table 3).

2.4. Structure solution and refinement

The structure of the complex of GTPSCS with CoA was solved by molecular replacement using the structure of dephosphorylated GTPSCS (PDB entry 1euc; Berman *et al.*, 2000; Fraser *et al.*, 2000) as a model. *PHENIX* (Adams *et al.*, 2010) and *Coot* (Emsley *et al.*, 2010) were used to refine the structure, and the model quality was judged using *MolProbity* (Chen *et al.*, 2010; Table 4).

3. Results and discussion

Electron density for CoA was evident in the initial electron-density maps (Fig. 1). CoA binds to the amino-terminal domain of the α-subunit of GTPSCS in an extended conformation (Fig. 2). Seven hydrogen bonds were identified between CoA and residues of GTPSCS, and four water

Figure 1
Initial electron density for CoA. The electron-density map ($F_o − F_c$, α_c) was calculated using the model of the $\alpha\beta$-dimer after molecular replacement and is contoured in green at the 3 r.m.s.d. level. The yellow ribbon diagram shows parts of the α-subunit, with N denoting its amino-terminus. The final model of CoA is shown as a stick model coloured according to atom type (purple, C; blue, N; red, O; yellow, S; orange, P) for verification.

molecules bridge between CoA and the α-subunit (Fig. 3a). The adenine base binds to two of these water molecules, but also makes hydrophobic interactions with Pro48α and Val80α packing against the two faces. A charged interaction has been identified between Lys50α and the 3′-phosphoryl group of CoA.

The adenosine and phosphate portions of CoA are well ordered, with clear electron density, but poorer electron density for the free thiol portion indicates that this portion is not well ordered. The conformation modelled is similar to that originally determined for the complex of *E. coli* SCS with CoA (Wolodko *et al.*, 1994). The electron-density maps suggest that a second conformation might exist, with the thiol of Cys132α flipped to the exterior and disulfide-linked to CoA. This conformation was observed in the complex of *E. coli* SCS with CoA and ADP–Mg^{2+} (Joyce *et al.*, 2000). Since the mitochondrial matrix would generally be maintained as a reducing environment, β-ME was used in the purification and the crystallization of GTPSCS to mimic this reducing environment. However, the oxidation of β-ME during crystallization may have led to formation of the disulfide between Cys132α and the thiol of CoA in some molecules of the crystal.

The protein has a very similar conformation to previous structures of phosphorylated and dephosphorylated pig GTPSCS without CoA (PDB entries 1euc and 1eud; Fraser *et al.*, 2000). Superposition with dephosphorylated GTPSCS without CoA (PDB entry 1euc) gives a root-mean-squared deviation (r.m.s.d.) of 0.44 Å based on 696 C$^\alpha$ atoms from the α- and β-subunits. When CoA binds, it displaces eight water molecules that have similar locations to the N6A, C2A, O2A,

P2A, O9P, N4P and S1P atoms of CoA (Fig. 3a). Also, the side chain of Gln27α rotates away from the CoA-binding site. As in the structure with PDB code 1euc, the active-site histidine residue His259α is not phosphorylated, presumably because the protein was not phosphorylated with GTP–Mg^{2+} before crystallization.

The interactions of CoA with GTPSCS are similar to those seen for CoA and *E. coli* SCS (PDB entry 2scu; Fraser *et al.*, 1999; Fig. 3b). Superposition with the complex of CoA bound to *E. coli* SCS gives an r.m.s.d. of 1.54 Å for 648 C$^\alpha$ atoms. Identical residues interact with CoA, with the exception that Ser18α in *E. coli* SCS is substituted by Lys26α in GTPSCS. Since CoA interacts with the amide NH of Ser18α or Lys26α, the difference in side chains has little impact.

In addition to succinyl-CoA synthetases, one other family of proteins has been found to bind CoA in an extended conformation at a Rossmann fold. This family consists of single-domain CoA-binding proteins (Hiyama *et al.*, 2006) that are similar to *E. coli* YccU (Wasinger & Humphery-Smith, 1998). Isothermal titration calorimetry has been used to measure the binding of CoA to one member of this family, TT1466 from *Thermus thermophilus* HB8 (Wada *et al.*, 2003). The value of $1.2 \pm 0.5 \times 10^5 \, M^{-1}$ is comparable to the apparent Michaelis

Figure 3
CoA interactions. (*a*) Superposition of GTPSCS bound to CoA with GTPSCS in the absence of CoA. (*b*) Superposition of GTPSCS bound to CoA with *E. coli* SCS bound to CoA. The C atoms of GTPSCS bound to CoA are yellow, while those of GTPSCS without CoA are magenta and those of *E. coli* SCS and its bound CoA are green. CoA is coloured as in Fig. 1.
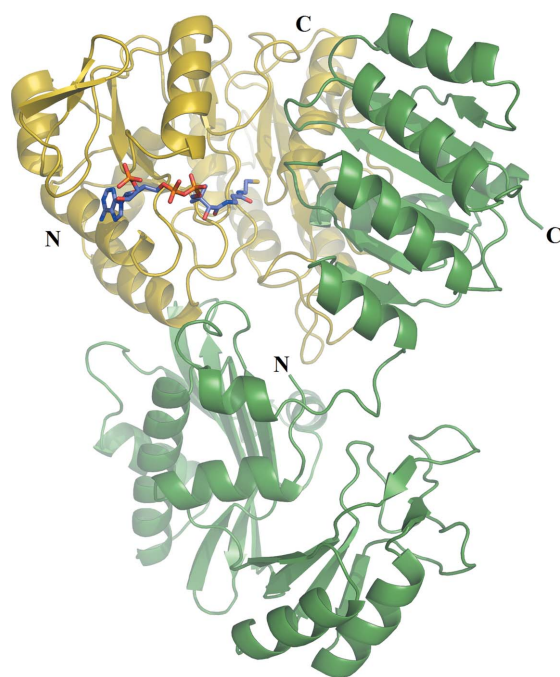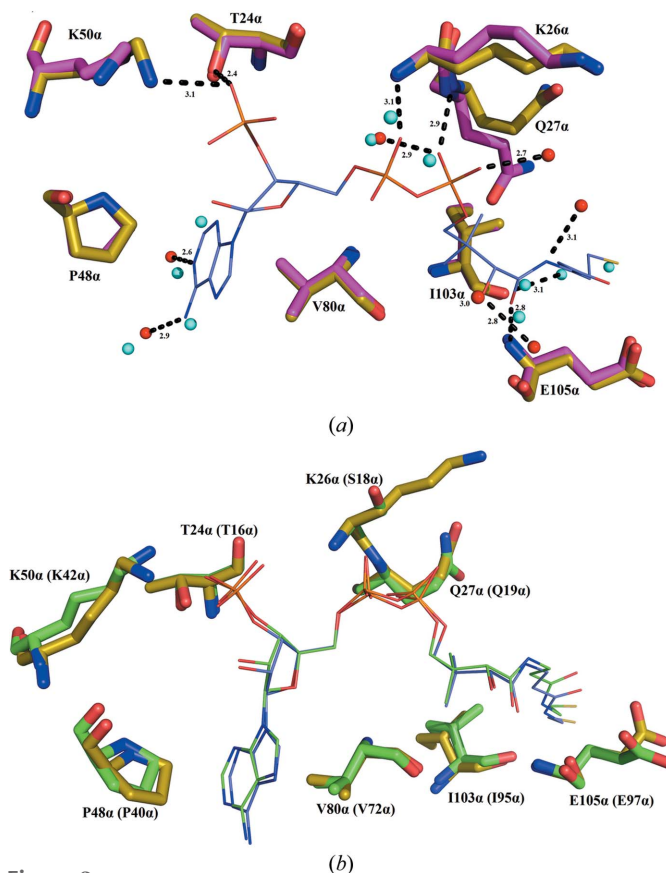
Figure 2
CoA bound to pig GTPSCS. CoA is shown as a stick model coloured as in Fig. 1. The α- and β-subunits are drawn as ribbon diagrams in yellow and green, respectively, with their termini labelled.

constant of *E. coli* SCS for CoA: $2.5 \times 10^5\ M^{-1}$ (Joyce *et al.*, 1999). X-ray crystallography showed that these single-domain CoA-binding proteins bind CoA at the Rossmann fold, although the path of the CoA is different from that in the complex with SCS from the 5′-phosphates to the free thiol (Hiyama *et al.*, 2006). Although the structural comparison of Hiyama and coworkers suggested that *E. coli* SCS uses both the α- and β-subunits to bind CoA, the interaction with the β-subunit is a crystal-packing interaction, not one that exists in solution. The fact that CoA only binds to the α-subunit is evident in the complex of CoA with GTPSCS.

References

Adams, P. D. *et al.* (2010). *Acta Cryst.* D**66**, 213–221.
Battye, T. G. G., Kontogiannis, L., Johnson, O., Powell, H. R. & Leslie, A. G. W. (2011). *Acta Cryst.* D**67**, 271–281.
Berman, H. M., Westbrook, J., Feng, Z., Gilliland, G., Bhat, T. N., Weissig, H., Shindyalov, I. N. & Bourne, P. E. (2000). *Nucleic Acids Res.* **28**, 235–242.
Bishop, D. F., Tchaikovskii, V., Hoffbrand, A. V., Fraser, M. E. & Margolis, S. (2012). *J. Biol. Chem.* **287**, 28943–28955.
Chen, V. B., Arendall, W. B., Headd, J. J., Keedy, D. A., Immormino, R. M., Kapral, G. J., Murray, L. W., Richardson, J. S. & Richardson, D. C. (2010). *Acta Cryst.* D**66**, 12–21.
Deng, J., Davies, D. R., Wisedchaisri, G., Wu, M., Hol, W. G. J. & Mehlin, C. (2004). *Acta Cryst.* D**60**, 203–204.
Elpeleg, O., Miller, C., Hershkovitz, E., Bitner-Glindzicz, M., Bondi-Rubinstein, G., Rahman, S., Pagnamenta, A., Eshhar, S. & Saada, A. (2005). *Am. J. Hum. Genet.* **76**, 1081–1086.
Emsley, P., Lohkamp, B., Scott, W. G. & Cowtan, K. (2010). *Acta Cryst.* D**66**, 486–501.
Fraser, M. E., Hayakawa, K., Hume, M. S., Ryan, D. G. & Brownie, E. R. (2006). *J. Biol. Chem.* **281**, 11058–11065.
Fraser, M. E., James, M. N. G., Bridger, W. A. & Wolodko, W. T. (1999). *J. Mol. Biol.* **285**, 1633–1653.
Fraser, M. E., James, M. N. G., Bridger, W. A. & Wolodko, W. T. (2000). *J. Mol. Biol.* **299**, 1325–1339.
Hamilton, M. L. & Ottaway, J. H. (1981). *FEBS Lett.* **123**, 252–254.
Hiyama, T. B., Zhao, M., Kitago, Y., Yao, M., Sekine, S.-I., Terada, T., Kuroishi, C., Liu, Z.-J., Rose, J. P., Kuramitsu, S., Shirouzu, M., Watanabe, N., Yokoyama, S., Tanaka, I. & Wang, B.-C. (2006). *J. Struct. Funct. Genomics*, **7**, 119–129.
Johnson, J. D., Muhonen, W. W. & Lambeth, D. O. (1998). *J. Biol. Chem.* **273**, 27573–27579.
Joyce, M. A., Fraser, M. E., Brownie, E. R., James, M. N. G., Bridger, W. A. & Wolodko, W. T. (1999). *Biochemistry*, **38**, 7273–7283.
Joyce, M. A., Fraser, M. E., James, M. N. G., Bridger, W. A. & Wolodko, W. T. (2000). *Biochemistry*, **39**, 17–25.
Lambeth, D. O., Tews, K. N., Adkins, S., Frohlich, D., & Milavetz, B. I. (2004). *J. Biol. Chem.* **279**, 36621–36624.
Murakami, Y. & Nishimura, J. S. (1974). *Biochem. Biophys. Acta*, **336**, 252–263.
Murzin, A. G. (1996). *Curr. Opin. Struct. Biol.* **6**, 386–394.
Ottaway, J. H., McClellan, J. A. & Saunderson, C. L. (1981). *Int. J. Biochem.* **13**, 401–410.
Sanadi, D. R., Gibson, D. M., Ayengar, P. & Jacob, M. (1956). *J. Biol. Chem.* **218**, 505–520.
Wada, T., Shirouzu, M., Terada, T., Ishizuka, Y., Matsuda, T., Kigawa, T., Kuramitsu, S., Park, S.-Y., Tame, J. R. H. & Yokoyama, S. (2003). *Acta Cryst.* D**59**, 1213–1218.
Wasinger, V. C. & Humphery-Smith, I. (1998). *FEMS Microbiol. Lett.* **169**, 375–382.
Winn, M. D. *et al.* (2011). *Acta Cryst.* D**67**, 235–242.
Wolodko, W. T., Fraser, M. E., James, M. N. G. & Bridger, W. A. (1994). *J. Biol. Chem.* **269**, 10883–10890.